ISSN 2413-5577, Ecological Safety of Coastal and Shelf Zones of Sea, 2026, No. 1, pp. 6–26.

Original paper

Experience in Monitoring Greenhouse Gas Emissions and Uptake in the Coastal Sea Zone

B. V. Divinsky *, S. B. Kuklev, V. V. Kremenetsky, A. A. Nedospasov, V. V. Ocherednik, O. N. Kukleva

Shirshov Institute of Oceanology, Russian Academy of Sciences, Moscow, Russia
* *e-mail: divin@ocean.ru*

Abstract
The study aims to monitor the emissions and uptake of carbon dioxide and water vapour at a specialized carbon polygon near the city of Gelendzhik, Krasnodar Krai. The paper analyses CO_2 and H_2O fluxes along with atmospheric parameters recorded from December 2024 to May 2025 using data from an automatic LI-COR Environmental monitoring station installed 25 m from the shoreline. Gas fluxes were calculated using the eddy covariance method at a frequency of 10 Hz. The main components of the station are atmospheric heat flux sensors, including a photosynthetically active radiation sensor; an ultrasonic anemometer; a gas analyzer; an air temperature and humidity sensor; soil temperature, heat flux and moisture content sensors; and a precipitation gauge. Daytime and nighttime partitioning of the net CO_2 flux into gross primary production and ecosystem respiration was applied. The results of the experiment showed that about 500 g of carbon dioxide per square meter was emitted into the atmosphere from the study area during the specified period. Ecosystem respiration accounted for 1300 g, whereas gross primary production accounted for 800 g. Seasonal dynamics of the exchange were identified: during winter months and in early calendar spring, CO_2 emission into the atmosphere prevails, while from April onward its uptake by the ecosystem is observed. The average CO_2 concentration in the air during the observation period was 423.2 ± 5.2 μmol/mol (with a global average of 420 μmol/mol). Despite the challenging conditions of the station's location in the coastal zone, the obtained results are physically sound and can be used to estimate greenhouse gas fluxes.

Keywords: carbon polygons, Gelendzhik, carbon dioxide flux, eddy covariance method, Li-Cor

Acknowledgements: The work was performed under state assignment topic no. FMWE-2023-0001 of Institute of Oceanology of RAS and funded by the Andrey Melnichenko Foundation.

For citation: Divinsky, B.V., Kuklev, S.B., Kremenetsky, V.V., Nedospasov, A.A., Ocherednik, V.V. and Kukleva, O.N., 2026. Experience in Monitoring Greenhouse Gas Emissions and Uptake in the Coastal Sea Zone. *Ecological Safety of Coastal and Shelf Zones of Sea*, (1), pp. 6–26.

Опыт мониторинга эмиссии и поглощения парниковых газов в прибрежной зоне моря

Б. В. Дивинский *, С. Б. Куклев, В. В. Кременецкий, А. А. Недоспасов, В. В. Очередник, О. Н. Куклева

Институт океанологии им. П.П. Ширшова РАН, Москва, Россия
* *e-mail: divin@ocean.ru*

Аннотация
Цель работы – мониторинг эмиссии и поглощения углекислого газа и водяного пара на специализированном карбоновом полигоне в районе г. Геленджика Краснодарского края. Проанализированы потоки CO_2 и H_2O, а также параметры состояния атмосферы, зарегистрированные с декабря 2024 г. по май 2025 г. с помощью автоматической станции мониторинга *LI-COR Environmental*, установленной в 25 м от береговой линии. Потоки газов рассчитывались методов турбулентных пульсаций с частотой 10 Гц. Основными компонентами станции являются: датчики потоков атмосферного тепла, включая датчик фотосинтетической активной радиации; ультразвуковой анемометр; газоанализатор; датчик температуры и влажности воздуха; почвенные датчики. Применялось дневное и ночное разделение чистого потока CO_2 на валовую первичную продукцию и экосистемное дыхание. Установлено, что за указанный период на исследуемом участке с квадратного метра в атмосферу поступило около 500 г углекислого газа. При этом на экосистемное дыхание пришлось около 1300 г, на валовую продукцию – 800 г. Выявлена сезонная динамика обмена: в зимние месяцы, а также в начале календарной весны преобладает эмиссия CO_2 в атмосферу, с апреля наблюдается его усвоение экосистемой. Средняя за период наблюдений концентрация CO_2 в воздухе составила 423.2 ± 5.2 мкмоль/моль (при среднемировой в 420 мкмоль/моль). Несмотря на сложные условия расположения станции в прибрежной зоне моря, полученные результаты физически обоснованы и могут использоваться для оценок потоков парниковых газов.

Ключевые слова: карбоновые полигоны, Геленджик, поток углекислого газа, метод турбулентных пульсаций, *Li-Cor*

Благодарности: работа выполнена в рамках темы государственного задания Института океанологии РАН № FMWE-2023-0001 при финансовой поддержке Фонда Мельниченко.

Для цитирования: *Дивинский Б. В., Куклев С. Б., Кременецкий В. В., Недоспасов А. А. и др.* Опыт мониторинга эмиссии и поглощения парниковых газов в прибрежной зоне моря // Экологическая безопасность прибрежной и шельфовой зон моря. 2026. № 1. С. 6–26. EDN PGBTAO.

Introduction

Greenhouse gases that determine the nature of climate change on the planet include water vapour H_2O, carbon dioxide CO_2, methane CH_4, nitrous oxide N_2O, and a group of fluorine-containing gases. Water vapour is the most abundant greenhouse gas in the atmosphere. Its contribution to the climatic fluctuations in air temperature [1)], according to various estimates, is 40–70%. At the same time,

[1)] Atmospheric concentration of greenhouse gases: technical documentation. U.S. Environmental Protection Agency, 2016. 16 p. URL: https://www.epa.gov/sites/default/files/2016-08/documents/ghg-concentrations_documentation.pdf [Accessed: 15 December 2025].

it is believed that human economic activities (such as land reclamation and deforestation) have only a small direct impact on H_2O concentrations. According to the latest bulletin of the World Meteorological Organization [2)], the most important greenhouse gas with a significant anthropogenic footprint is carbon dioxide. Over the period from 1750 (approximately the pre-industrial era) to 2023, the CO_2 share of the anthropogenic temperature increase was about 66%. For comparison: the share of CH_4 was 16%, and that of N_2O was 6%. The global average concentration of carbon dioxide in the atmosphere in 2023 was 420.0 ± 0.1 μmol/mol, with the average growth rate over the last decade reaching 2.4 μmol/mol per year.

In the Russian Federation, research on greenhouse gas fluxes has been developing quite intensively in recent years [1–8]. In 2023, a monograph [9] was published summarizing balance estimates of fluxes of the main greenhouse gases in Russia and concluding that the so-called forest regions of the country (Siberian, Far Eastern, etc.) are net sinks of greenhouse gases, while emission sources are the southern regions with a predominance of pastures and agricultural lands (Southern, North Caucasian, Volga).

In 2021, within the framework of the national system for monitoring greenhouse gas dynamics, the Ministry of Science and Higher Education of the Russian Federation launched the "Carbon Polygons" project (URL: https://carbon-polygons.ru), within which monitoring observations are carried out at nineteen separate sites located in various natural zones of Russia (steppes, taiga forests, swamps, pastures, agricultural lands, forest-tundra). The main task of the carbon polygons is to conduct long-term and, crucially, continuous measurements of greenhouse gas fluxes using modern instrumentation. One such polygon is the measuring site in the area of Gelendzhik, Krasnodar Krai.

Despite the expanding observation network, there is still a lack of detailed data on greenhouse gas fluxes for the coastal resort zones of the Black Sea based on direct instrumental measurements. The features of relief, soils, vegetation, and proximity to the sea form a unique coastal ecosystem whose carbon balance remains poorly understood.

This work aims at studying the fluxes of carbon dioxide and water vapour at the Gelendzhik carbon polygon from December 2024 to May 2025.

Materials and Methods

Gelendzhik carbon polygon. The Gelendzhik polygon, with a total area of 26 hectares, consists of terrestrial and marine parts, where regular instrumental observations of carbon dioxide, water vapour, and methane fluxes, as well as associated atmospheric state parameters, have been conducted since 2022 [10–12].

[2)] The state of greenhouse gases in the atmosphere based on global observations through 2023. Geneva : WMO, 2024. 11 p. (WMO Greenhouse Gas Bulletin ; No. 20). Available at: https://library.wmo.int/idurl/4/69057 [Accessed: 15 December 2025].

According to soil-ecological zoning [3)], the Gelendzhik area is located within the Novorossiysk district of the Western Brown Earth-Forest soil-bioclimatic region of the subboreal geographical belt. The soil cover here is mainly represented by acidic podzolized brown earths and calcareous soddy soils. The herbaceous layer is mainly formed by sheep fescue and heath false brome. Among the plants found are butcher's-broom (sp), three-leaf jasmine (sp), Anatolian blackberry (cop1), and resinous psoralea (un). Coastal vegetation is also represented by Pitsunda pine with an average crown attachment height of 8–9 m, downy oak, growing singly or in clumps, with an average age of about 12 years, as well as hornbeam, dog's bramble, Christ's thorn, and juniper.

In November 2024, the measuring part of the polygon was supplemented with an automatic monitoring station based on the LI-7200 gas analyzer (LI-COR Environmental, USA). The installation is operated by the Southern Branch of the Shirshov Institute of Oceanology, Russian Academy of Sciences. The station is mounted on open natural soil 7 m from a rocky cliff and 25 m directly from the shoreline (Fig. 1). Station coordinates: 44.576657° N, 37.977450° E.

The main components of the station (Fig. 2) are:

1. LI-7550 interface Module (a universal component of all gas measurement systems, containing integrated tools for digital signal processing from gas analyzers).

F i g . 1 . Location of the LI-COR monitoring station at the Gelendzhik polygon

[3)] Information system "Soil-Geographic Database of Russia": [website]. Available at: https://soil-db.ru [Accessed: 15 December 2025] (in Russian).

F i g . 2 . Measuring instruments of the LI-COR monitoring station: *1* – LI-7550 interface module; *2* – atmospheric heat flux sensors, including a photosynthetically active radiation sensor; *3* – ultrasonic anemometer; *4* – gas analyser; *5* – air temperature and humidity sensor; *6* – soil temperature, heat flux and moisture content sensors; *7* – precipitation gauge

2. Atmospheric heat flux sensors, including photosynthetically active radiation sensors (Kipp&Zonen, Netherlands and LI-190R).

3. uSonik-3 ultrasonic anemometer (Metek, Germany).

4. LI-7200 gas analyzer.

5. HMP155 air temperature and humidity sensor (Vaisala, Finland).

6. HydraProbe (Stevens Water Monitoring Systems, USA) and Hukseflux (Hukx, Netherlands) soil temperature, heat flux, and moisture content sensors.

7. TR-525M precipitation gauge (Texas Electronics, USA).

The LI-7200 gas analyzer determines the molar fractions of water vapour and carbon dioxide in an air sample with an accuracy of 2% and 1% of reading, respectively. The station is powered from the laboratory building. The station is connected to a server for acquisition, accumulation and storage of measurement data. The sensor interrogation frequency of the measuring equipment is 10 Hz. All data are processed by standard software and stored on the server.

The data obtained from the station form three separate arrays:

1. Half-hourly data arrays with a sampling interval of 0.1 s (total 18,000 values), containing values of atmospheric carbon dioxide CO_2 and water vapour H_2O, atmospheric pressure, air temperature, and three wind speed components.

2. Processed data arrays with a 1-minute resolution, including the following characteristics: surface albedo; incoming and outgoing shortwave and longwave radiation; Photosynthetic Photon Flux Density (*PPFD*); precipitation amount; air temperature and relative humidity; soil moisture content and temperature; Soil Heat Flux (*SHF*).

3. Statistical parameters characterizing the atmosphere and soil state, obtained by processing the 30-minute raw data. The parameters include: mean values, variance, and higher moments (skewness, kurtosis) of the distributions of three wind speed components (two horizontal and one vertical), carbon dioxide and water vapour concentrations, soil temperature; mean values of surface albedo, incoming and outgoing shortwave and longwave radiation, *PPFD*, precipitation, air humidity and temperature, soil moisture content and temperature, *SHF*; mean values of sensible and latent heat fluxes, carbon dioxide and water vapour fluxes; mean atmospheric state parameters (temperature, humidity, pressure, wind speed and direction, estimate of turbulent kinetic energy, Bowen ratio); estimates of covariance between greenhouse gas fluxes and main meteorological parameters.

The software (EddyPro) allows for correcting flux estimates based on the analysis of outliers, airflow stability, trend components, and time delays of measuring equipment.

Greenhouse gas flux calculations

Eddy covariance method. Currently, the most common and theoretically sound method for calculating greenhouse gas fluxes is the eddy covariance method. The basic principles of the method are outlined in guidelines [4), 5)] and are as follows. The turbulent vertical flux of any substance (e.g., greenhouse gas) can be represented as the covariance of the vertical wind speed and the concentration of that substance. The high frequency of turbulent fluctuations typical of the atmosphere imposes increased requirements on the recording equipment and the operating frequency of sensors (10 Hz in our case). Important limitations of the method are the following assumptions: 1) air density fluctuations are small and can be neglected; 2) over the measurement period (30 min), vertical air mass movements are insignificant. In real natural conditions, especially in areas with complex terrain, these conditions are not always met, which leads to natural errors and measurement uncertainties.

Footprint. An important parameter of the eddy covariance method is so-called footprint – the spatial area from which fluxes are recorded by the station's instruments. The footprint estimate depends on many factors: the height of the instrument installation (4 m in our case), surface roughness, and the nature of atmospheric stratification. The horizontal extent of the footprint, defined as the distance upwind from the sensor installation point, is described statistically in terms of distribution quantiles.

[4)] Aubinet, M., Vesala, T. and Papale, D., eds., 2012. Eddy Covariance: A Practical Guide to Measurement and Data Analysis. Springer Science+Business Media B.V., 438 p. https://doi.org/10.1007/978-94-007-2351-1

[5)] Burba, G.G., Kurbatova, Yu.A., Kuricheva, O.A., Avilov, V.K., etc., 2016. Eddy Covariance Method. Brief Practical Guide. Moscow: A.N. Severtsov Institute of Ecology and Evolution RAS, 223 p. (in Russian).

For example, the 80% footprint is the length (in meters) of the area from which the contribution of a given substance (CO_2 in our case) to the flux is 80%.

Flux partitioning. Carbon dioxide flux calculated by the eddy covariance method represents the Net Ecosystem Exchange (*NEE*) and can be partitioned into the two largest components of the carbon cycle: Gross Primary Production (*GPP*) and ecosystem respiration (R_{eco}). Gross primary production is the total amount of organic matter created by autotrophic organisms during photosynthesis (more precisely, chemosynthesis). *GPP* thus reflects the amount of carbon absorbed by plants during photosynthesis. Ecosystem respiration is associated with the processes of converting organic carbon into CO_2 by organisms and acts as the main pathway for carbon release from terrestrial ecosystems into the atmosphere. In general form, $NEE = R_{eco} - GPP$.

Flux partitioning was performed according to the recommendations outlined in [13]. Currently, several partitioning methods exist. The two most widely used alternative approaches are the so-called nighttime and daytime partitioning:

1. In nighttime partitioning [14], R_{eco} is estimated during nighttime and subsequently extrapolated to the daylight hours. *GPP* is calculated as the difference between R_{eco} and *NEE*. In this case, the stochastic nature of turbulence and noise in the measurement signals can lead to negative *GPP* flux estimates, even though they are positive by definition. However, negative *GPP* fluxes should not be removed (or set to zero), as this would lead to a significant bias in the overall estimates of gross primary production.

2. Daytime partitioning [15] is based on model estimates of NEE_{mod} using light response curves, assuming proportionality between carbon dioxide fluxes and incoming radiation. Given the uncertainty and error of model approximations of fluxes, the resulting model flux, calculated as the difference ($R_{eco} - GPP$), may not exactly match the measured *NEE* value.

An important detail should be noted. Since the natural system is complex and multifactorial, data on primary production and ecosystem respiration fluxes obtained for a specific period are likely to contain significant uncertainty. However, when processed statistically over a long period (months, years), these data will quite correctly reflect the balance components of carbon cycle of the ecosystem under consideration.

Data quality. A key assumption of the eddy covariance method is the stationarity of the mean flow (spatial homogeneity). The initial data quality is assessed according to the approach outlined in [16]. The initial 30-minute observation series is divided into six 5-minute segments. For each segment, the covariance between vertical velocity fluctuations and the parameter under study is calculated.

The flux is considered stationary if the covariances for the individual segments differ from the covariance calculated for the entire series by no more than 30%. Overall, a flag is assigned to each series indicating the quality of the measurements:

– flag 0 (deviation < 30%) – high-quality data;

– flag 1 (deviation < 100%) – medium-quality data but suitable for use in long-term research programs;

– flag 2 (deviation > 100%) – low-quality data to be excluded from analysis.

The proportion of series with low-quality data (flag 2) for carbon dioxide fluxes by month is as follows: December – 22%, January – 15%, February – 26%, March – 21%, April – 19%, May – 22%. Thus, on average across months, about 20% of data are deemed unfit for use due to poor quality, resulting in gaps in the overall time series. The continuity of the time series is achieved by artificially filling these gaps using algorithms described in [13].

Results and Discussion

The main parameters used to estimate the integral values of greenhouse gas emissions (or uptake) are: carbon dioxide flux, sensible and latent heat fluxes, incoming shortwave radiation flux, air and soil temperature, relative humidity, water vapour pressure deficit, and characteristics of the wind flow (wind speed, wind direction, friction velocity, Monin – Obukhov length for turbulent flow).

Fig. 3–5 presents the temporal dynamics of some atmospheric parameters, as well as the carbon dioxide and water vapour content measured over the six-month experimental period.

As follows from Fig. 3, a steady increase in the photosynthetic photon flux density, necessary for photosynthesis, is observed from the end of January. With the onset of calendar spring (March), the soil gradually warms up, and the sign of *SHF* becomes positive. Negative average daily air temperatures were recorded only in the second half of February. Fig. 3 presents the seasonal dynamics of key abiotic factors determining the ecosystem's carbon exchange. Analysis of average daily values shows that from the end of January, a steady increase in *PPFD* is observed, which creates prerequisites for the start of active vegetation. Soil warming, indicated by the change in the SHF sign to positive, becomes stable from March, coinciding with the onset of calendar spring. At the same time, periods with negative average daily air temperature T_a values were noted only in the second half of February. The dynamics of soil temperature T_s corresponded to changes in air temperature and radiation balance. This comprehensive dataset serves as a basis for subsequent analysis of the driving forces and seasonal dynamics of greenhouse gas fluxes.

The distribution of atmospheric precipitation by month during the observation period is uneven (Fig. 4).

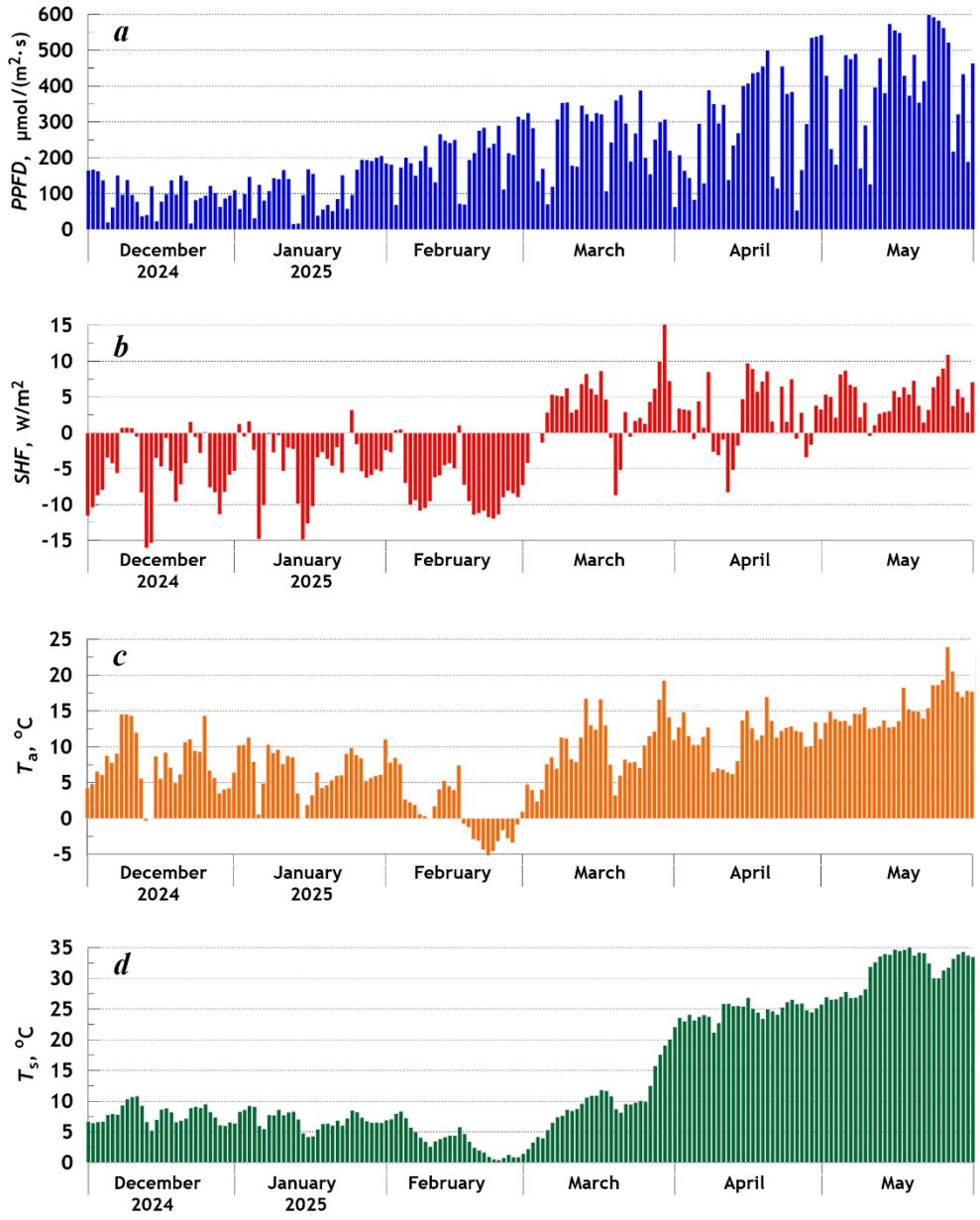

Fig. 3. Daily average values of photosynthetic photon flux density *PPFD*, soil heat flux *SHF*, air temperature T_a and soil temperature T_s from December 2024 to May 2025

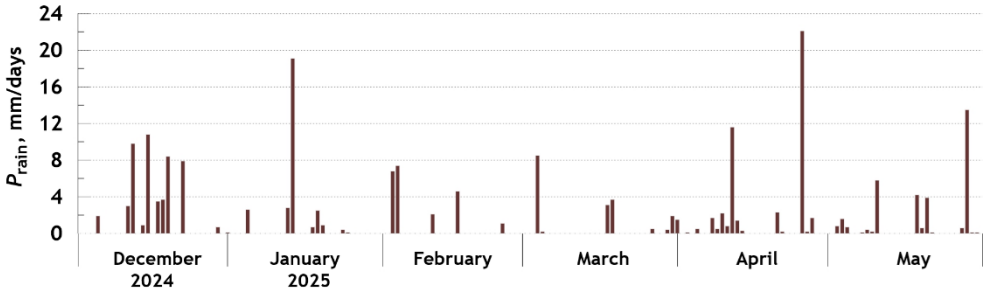

F i g . 4 . Daily atmospheric precipitation values from December 2024 to May 2025

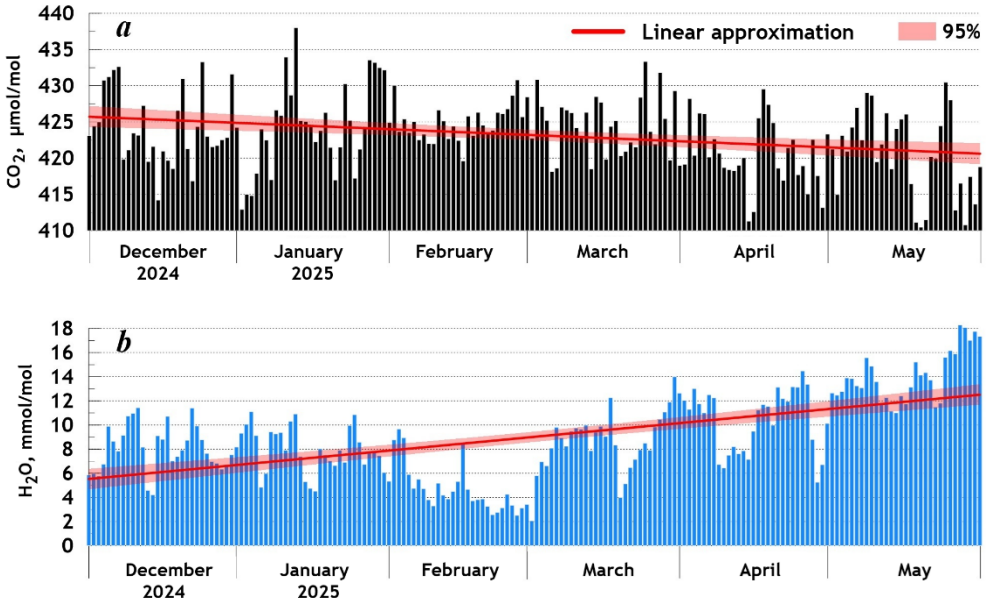

F i g . 5 . Daily average concentrations of carbon dioxide and water vapour in the atmosphere from December 2024 to May 2025. The red line represents linear approximation, the pink area shows the 95% confidence interval for the regression line

Total monthly precipitation values were (climatic norms according to the Unified State System of Information on the Situation in the World Ocean [6]) are given in parentheses): December – 50.7 mm (60.1 mm); January – 29.1 mm (40.4 mm); February – 22.0 mm (31.8 mm); March – 19.8 mm (32.3 mm); April – 45.6 mm (30.7 mm); May – 32.7 mm (31.6 mm). December was the wettest month, although precipitation was somewhat below climatological values. January, February, and March were abnormally dry; in April, precipitation exceeded the norm by 1.5 times; May was characterized by average values.

The maximum carbon dioxide content (Fig. 5) was observed in February (437.8 μmol/mol), and the minimum in May (410.5 μmol/mol).

The highest water vapour concentrations were recorded in May (18.1 mmol/mol), the lowest in March (1.9 mmol/mol). The average CO_2 concentration in the air over the observation period was 423.2 ± 5.2 μmol/mol (compared to the global average of 420 μmol/mol), and for H_2O it was 9.0 ± 3.6 mmol/mol. From December to May, a steady negative trend in average daily carbon dioxide concentrations and a positive trend in water vapour were observed. Such seasonal dynamics are typical for all territories with seasonal changes in key atmospheric parameters and vegetation cover, which determine air temperature and photosynthetic activity.

Fig. 6 presents monthly wind roses, characterizing the frequency of average wind speeds across 45-degree directional sectors.

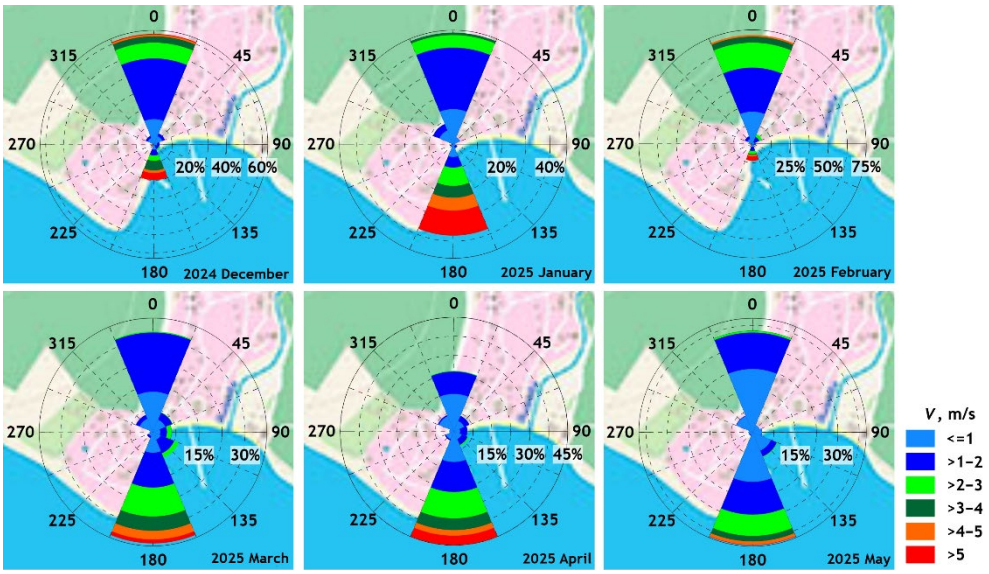

F i g . 6 . Wind speed frequency V (%) by directions in the experiment area

[6] Unified State System of Information on the Situation in the World Ocean (ESIMO). URL: www.esimo.ru (date of access: 10.12.2025) (in Russian).

As follows from Fig. 6, the wind regime is characterized by two pronounced directional sectors: northern and southern. In December and February, winds from northern directions dominated (60% and 73% frequency, respectively), in April – those from southern directions (45% frequency). In January, northern winds slightly prevailed, while in March and May – the southern ones. The average monthly and maximum wind speeds in December were 1.8 and 20.0 m/s, respectively; in January – 2.1 and 17.1 m/s; in February – 1.7 and 18.9 m/s; in March – 1.5 and 15.7 m/s; in April – 1.5 and 18.5 m/s; in May – 1.0 and 12.7 m/s. Despite the fact that climatically the strongest winds in the region are the northern ones (Novorossiysk bora), during the period under review, winds from southern directions exhibited the highest speeds.

The calculated flux footprint areas (Fig. 7) generally reflect the wind conditions discussed above. The footprint is elongated in the meridional direction

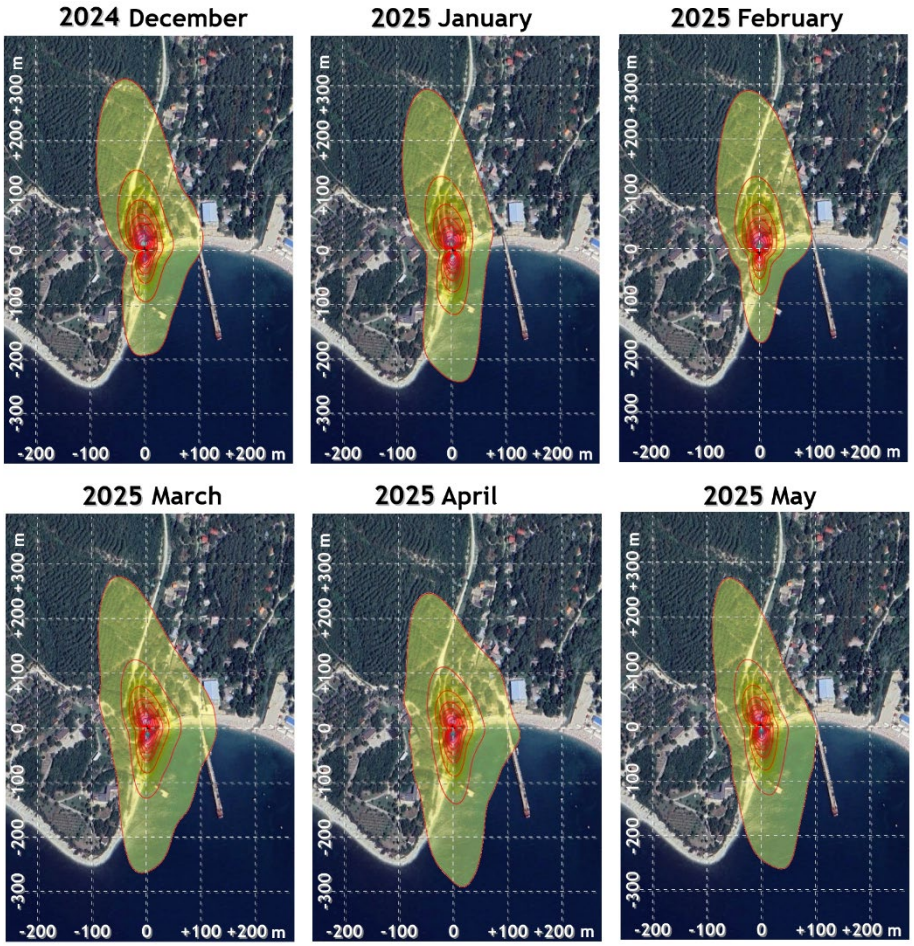

F i g . 7 . Monthly flux footprint coverage areas. Isolines are drawn for 10, 20, …, 90th percentiles of the distributions

(north – south). The average distance contributing most to the measured flux was 60 m from the measuring station, while the distance covering 90% of the contribution (90th percentile) reached 175 m. The monthly average footprint area thus amounts to about 11,000 m² of the underlying surface. In December and February, the footprint extends significantly to the north. In March and May, the footprint expands to the southeast, following the increasing frequency of southeast winds.

Fig. 8 and 9 show the diurnal dynamics of water vapour fluxes and fluctuations in net ecosystem exchange *NEE*, respectively, averaged by month. The graphs show the mean values, 95% confidence intervals for the mean, and the medians of the distributions. Differences between mean and median values indicate deviations of flux distributions from normality. The discrepancies are particularly pronounced in winter months, possibly due to difficulties in interpreting measurement results during this period. Nevertheless, the behavior of mean and median curves generally coincides.

Water vapour fluxes reach their daytime peak from 10:00 to 16:00 in winter; with the onset of spring, the peak period expands. A second maximum of water vapour fluxes, occurring at night (23:00–01:00), is noteworthy, and is discernible in December and (more weakly) in January.

Winter months are characterized by a prevailing emission of carbon dioxide into the atmosphere (Fig. 9) with a relatively weak diurnal cycle.

Starting in March, a stable diurnal cycle of CO_2 flux fluctuations is established: during the daytime, carbon dioxide is actively absorbed, and at night it is released. In May, the time range of carbon dioxide uptake is about 12 hours (from 6:00 to 18:00). The largest CO_2 emission was observed in December, and the largest

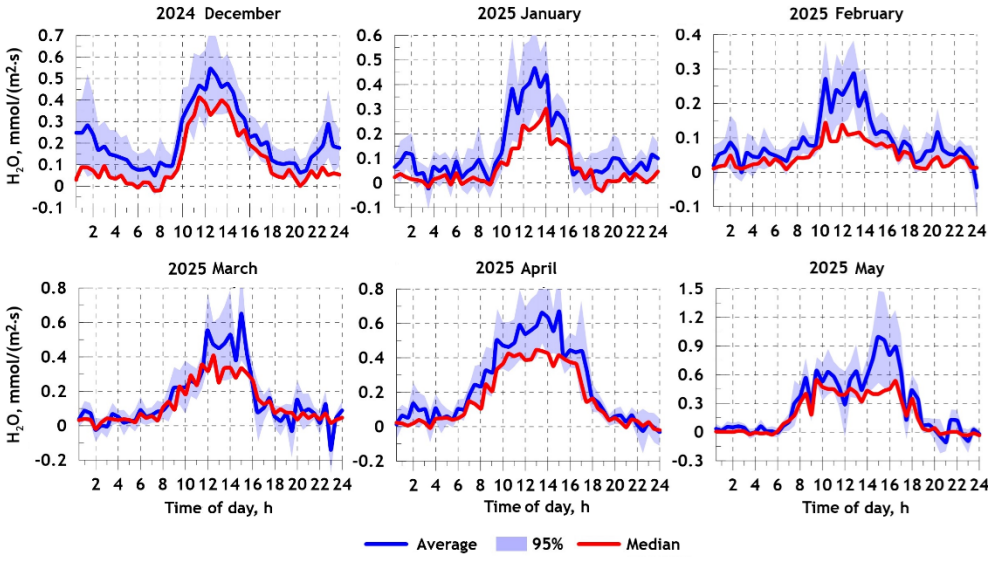

Fig. 8. Diurnal water vapour fluxes

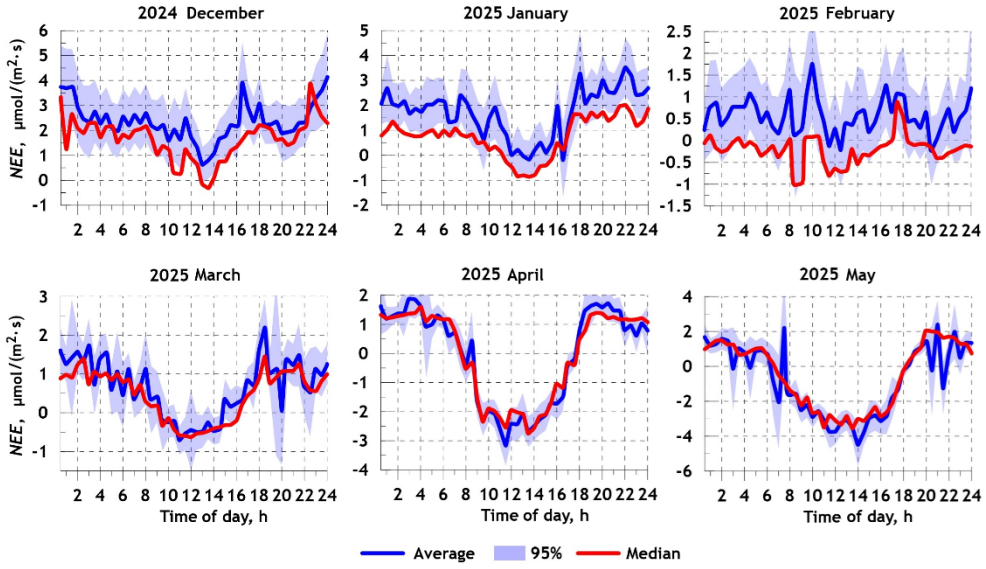

Fig. 9. Diurnal carbon dioxide fluxes

uptake in May, with characteristic flux values of 4–5 and 3–4 μmol/m²·s, respectively. Diurnal fluctuations in water vapour and carbon dioxide fluxes are noted by almost all researchers (e.g., in studies [17–19]). These fluctuations are driven by air temperature and photosynthetic activity. Naturally, the parameters of these fluctuations (amplitude, timing of peaks) depend on many other factors related to soil moisture, the state of the underlying surface, and atmospheric conditions.

As already mentioned, the carbon dioxide flux *NEE* can be partitioned into two important components of the carbon cycle, namely gross primary production *GPP* and ecosystem respiration R_{eco}; the graphs of their diurnal fluctuations are shown in Fig. 10. *GPP* and R_{eco} estimates are calculated using two alternative methods associated with daytime and nighttime partitioning of carbon dioxide fluxes.

Thus, gross primary production *GPP* quantifies the photosynthetic uptake of carbon by the ecosystem. Positive extremes of *GPP* correspond to maximum uptake of carbon dioxide by the ecosystem. In the context of ecosystems, negative respiration R_{eco} refers to the uptake of carbon dioxide, while positive respiration refers to its release. Recall: in the nighttime partitioning scheme, ecosystem respiration R_{eco} is modeled, and gross primary production *GPP* is calculated as the difference between R_{eco} and *NEE*. In daytime partitioning, both *GPP* and R_{eco} are modeled. In this case, the resulting model ecosystem exchange, calculated as $NEE_{mod} = R_{eco}(\text{day}) - GPP(\text{day})$, considering the inevitable modeling error, will differ from the experimentally measured *NEE*.

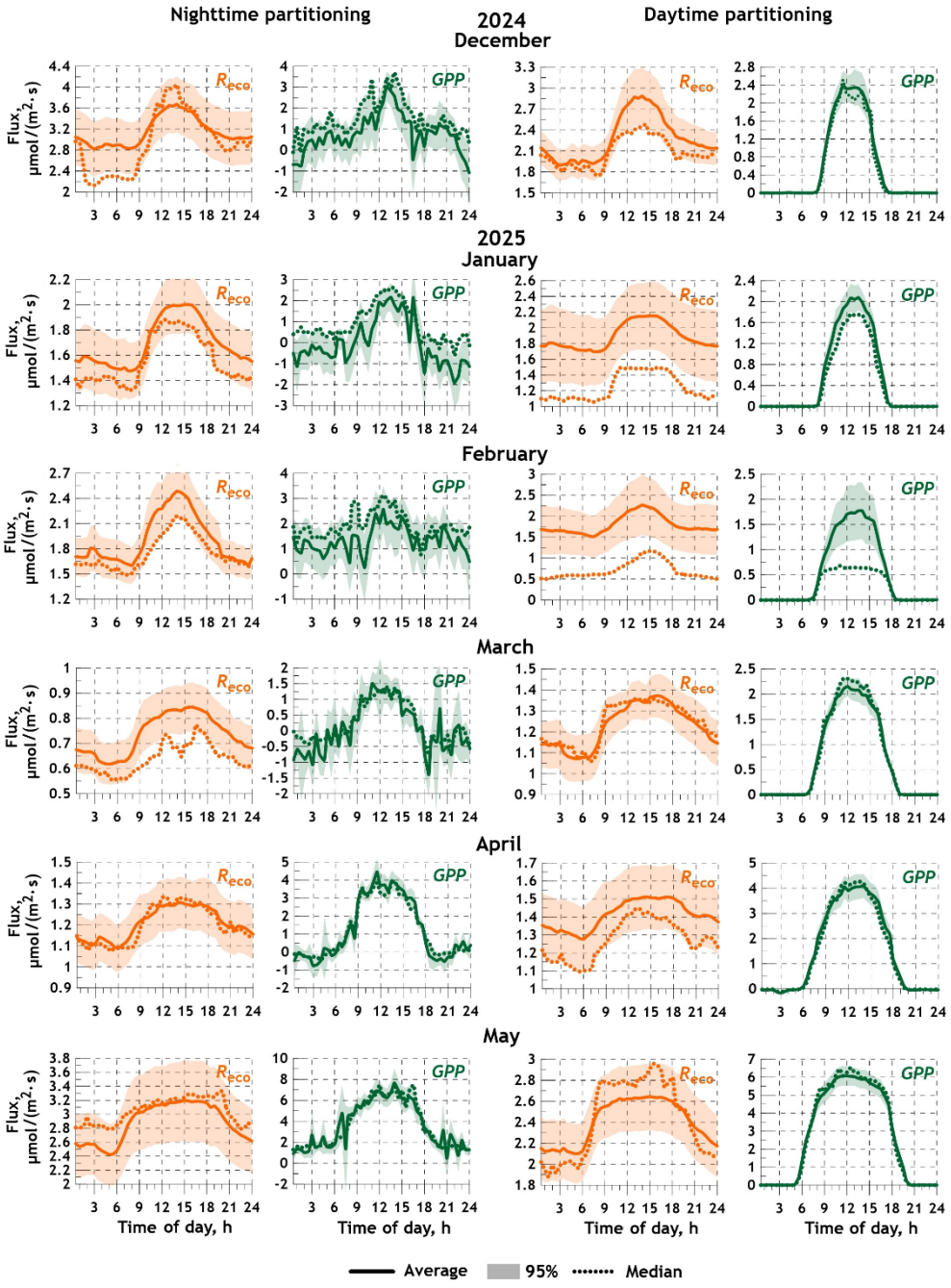

Fig. 10. Diurnal fluxes of gross primary production *GPP* and ecosystem respiration R_{eco} (the solid line is average, the dotted line is median, the shaded area is 95% confidence interval)

In Fig. 10, the second peak of ecosystem respiration occurring at night is quite remarkable. The stepped shape of the *GPP* curve in the daytime partitioning scheme is noteworthy, due to the features of the algorithmic approximation based on light-response curves. Nevertheless, with the onset of calendar spring and the intensification of photosynthesis, the "daytime" and "nighttime" *GPP* estimates show satisfactory agreement, especially in April and May.

Fig. 11 and 12 present the total daily and total monthly masses of carbon dioxide emitted into the atmosphere or absorbed from the atmosphere, respectively. The calculations were performed using the nighttime flux partitioning scheme.

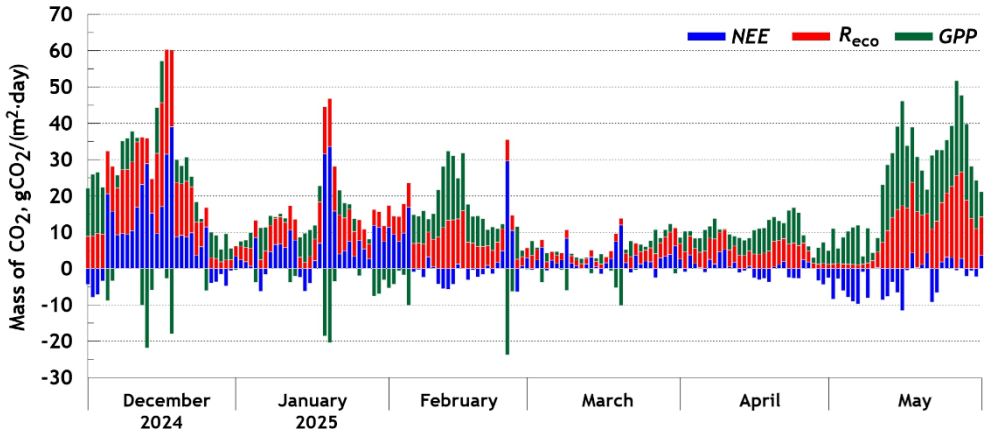

Fig. 11. Daily masses of carbon dioxide corresponding to net ecosystem exchange *NEE*, gross primary production *GPP* and ecosystem respiration R_{eco}

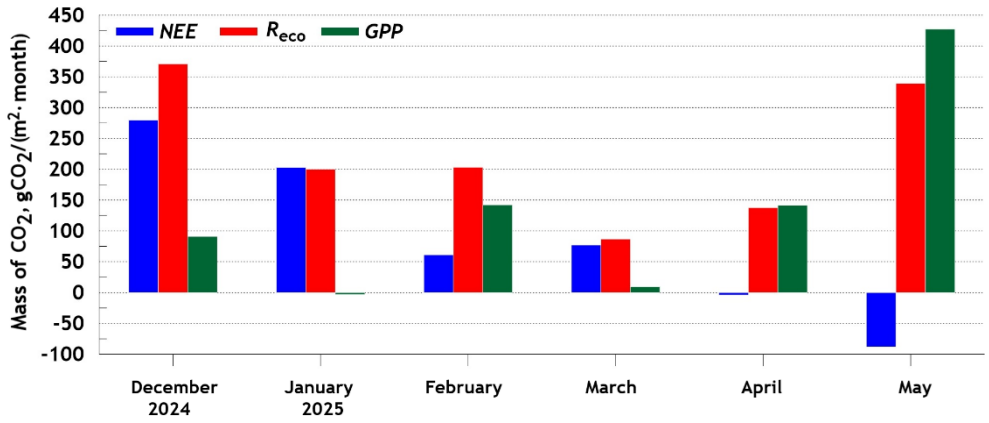

Fig. 12. Total monthly masses of carbon dioxide corresponding to net ecosystem exchange *NEE*, gross primary production *GPP* and ecosystem respiration R_{eco}

Thus, from December to March, CO_2 emission into the atmosphere was observed. Net ecosystem exchange *NEE* in December amounted to 278 $gCO_2/(m^2 \cdot month)$, in March – 76 $gCO_2/(m^2 \cdot month)$. From April onwards, a tendency towards atmospheric carbon dioxide uptake was observed, which reached 88 $gCO_2/(m^2 \cdot month)$ in May.

In total, over the six months of measurements, the net volume of carbon dioxide emissions *NEE* amounted to 529 gCO_2/m^2. Ecosystem respiration accounted for R_{eco}(night) = 1338 gCO_2/m^2, and gross primary production accounted for *GPP*(night) = 809 gCO_2/m^2.

Estimates obtained using the daytime flux partitioning scheme demonstrate comparable results: R_{eco}(day) = 1271 gCO_2/m^2, *GPP*(day) = 768 gCO_2/m^2. These values yield a model estimate of *NEE*(day) = 503 gCO_2/m^2.

Thus, the experimental value of total emissions (*NEE*) for the six months was 529 gCO_2/m^2, while the model value was 503 gCO_2/m^2. The close values suggest the correctness of the measurements and calculations performed.

As a small addition, we are to examine the fluctuations of carbon dioxide and water vapour fluxes in the frequency domain. Fig. 13 shows the frequency spectra of these fluctuations.

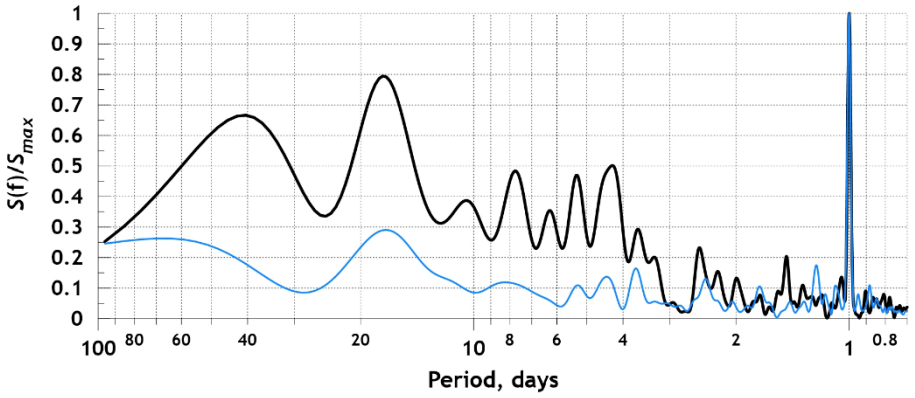

Fig. 13. Normalized spectra of carbon dioxide (black curve) and water vapour (blue curve) concentration fluctuations

For ease of comparison, the spectra are normalized to the spectral density values corresponding to the peak frequencies. Note also that the spectra are constructed from smoothed raw data, which eliminates fluctuation components. As follows from Fig. 13, two periods dominate the spectra of greenhouse gas flux fluctuations: diurnal (24 h) and a period of 17.2 days. For the CO_2 spectrum, these periods are comparable in amplitude, whereas in the H_2O fluctuation spectrum, the diurnal cycle is clearly dominant. Fluctuations in carbon dioxide fluxes on synoptic (several days) and seasonal (about 40 days) variability scales are of independent interest but require more detailed study and will form the subject of a separate task.

Conclusion

In light of the adoption in 2025 of the new national project "Ecological well-being" in Russia, research on greenhouse gas fluxes is an important not only ecological but also economic, social, and political task. At the same time, direct instrumental measurements of fluxes are far from trivial. The eddy covariance method used in this work imposes several significant limitations on the experimental conditions. Here we point out only the most important ones: 1) the site under consideration must be spatially homogeneous, without natural or artificial obstacles; 2) the energy balance (including sensible and latent heat fluxes, as well as soil fluxes) must be closed. Literal adherence to these conditions is practically unattainable, especially in areas of intense economic activity. Vast steppe (or tundra) areas may meet the first condition, but even for them, the energy balance will most likely be unclosed due to unaccounted advective heat fluxes, internal sources or vertical currents associated with uneven surface heating.

Despite the undeniable problematic aspects, we note that the greenhouse gas monitoring station in Gelendzhik is located on a typical site in the resort zone of the Krasnodar Krai Black Sea coast. Measurements at such sites seem necessary from both a scientific and practical point of view. The Gelendzhik carbon polygon is essentially the first experience of measurements under such conditions. Furthermore, the experimental results are based not on single (random) measurements but on long-term continuous data, which lends them a certain statistical reliability. Let us add that currently the eddy covariance method is successfully applied not only to natural environments but also to urban settlements. For example, study [20] uses greenhouse gas measurement data obtained from two stations located directly within the city limits of Basel (Switzerland).

Let us point out the main results obtained:

1. The measuring station of Gelendzhik polygon, operating since December 2024, automatically records the fluxes of the main greenhouse gases, as well as atmospheric state variables. The station is part of the Russian greenhouse gas monitoring project.

2. Based on the experimental results, it was found that from December 2024 to May 2025, about 500 g of carbon dioxide per square meter was emitted into the atmosphere from the study area. Ecosystem respiration accounted for about 1300 g, and gross primary production for 800 g.

3. Seasonal dynamics of carbon exchange were revealed: in the winter months, as well as at the beginning of calendar spring, CO_2 emission into the atmosphere prevails; from April onwards, its uptake by the ecosystem is observed.

Summing up, we note that despite a certain questionability of the station's location, the obtained results can be interpreted from a physical point of view. In particular, the diurnal and seasonal cycle of water vapour and carbon dioxide content agrees well with generally accepted concepts. This confirms the correctness of

the obtained data and the promise of instrumental measurements of greenhouse gas fluxes under complex conditions with further improvement of data processing methods.

The continuation of the experiment and, most importantly, obtaining continuous data will allow for further analysis of greenhouse gas fluxes and associated meteorological elements over a wide range of temporal variability, including seasonal and interannual fluctuations.

References

1. Zamolodchikov, D.G., Gytarsky, M.L., Shilkin, A.V., Marunich, A.S. and Karelin, D.V., 2017. Monitoring of Carbon Dioxide and Water Vapor Cycles at the Log Tayozhny Experimental Site (National Park Valdaysky). *Fundamental and Applied Climatology*, 1, pp. 54–68. https://doi.org/10.21513/2410-8758-2017-1-54-68 (in Russian).
2. Khoruzhy, D.S., 2018. Variability of the CO_2 Flux on the Water-Atmosphere Interface in the Black Sea Coastal Waters on Various Time Scales in 2010–2014. *Physical Oceanography*, 25(5), pp. 401–411. https://doi.org/10.22449/1573-160X-2018-5-401-411
3. Krivenok, L.A., Suvorov, G.G., Avilov, V.K. and Sirin, A.A., 2019. Eddy Covariance Measurement of CO_2, CH_4, and H_2O Fluxes: Use of a Mobile Tower and Taking into Account the Changing Fetch. *Optika Atmosfery i Okeana*, 31(11), pp. 942–950. https://doi.org/10.15372/AOO20191111 (in Russian).
4. Fedorov, Yu.A., Sukhorukov, V.V. and Trubnik, R.G., 2021. Review: Emission and Absorption of Greenhouse Gases by Soils. Ecological Problems. *Anthropogenic Transformation of Nature*, 7(1), pp. 6–34. https://doi.org/10.17072/2410-8553-2021-1-6-34 (in Russian).
5. Satosina, E., Zyrianov, V., Prokushkin, A. and Olchev, A., 2022. Temporal Variability of Carbon Dioxide, Methane, Sensible and Latent Heat Fluxes in Forest and Moore Cosystems of Northen Eurasia. *Grozny Natural Science Bulletin*, 7(4), pp. 79–85. https://doi.org/10.25744/genb.2022.41.14.010 (in Russian).
6. Mamkin, V., Avilov, V., Ivanov, D., Varlagin, A. and Kurbatova, J., 2023. Interannual Variability in the Ecosystem CO2 Fluxes at a Paludified Spruce Forest and Ombrotrophic Bog in the Southern Taiga. *Atmospheric Chemistry and Physics*, 23(3), pp. 2273–2291. https://doi.org/10.5194/acp-23-2273-2023
7. Orekhova, N.A., Medvedev, E.V., Mukoseev, I.N. and Garmashov, A.V., 2024. Sea-Air CO_2 Flux in the Northeastern Part of the Black Sea. *Ecological Safety of Coastal and Shelf Zones of Sea*, (1), pp. 57–67.
8. Panov, A.V., Makhnykina, A.V., Urban, A.V., Zyryanov, V.I., Polosukhina, D.A., Kukavskaya, E.A., Aryasov, V.E., Kolosov, R.A., Putilin, I.R. et al., 2024. Carbon Flows in the Ecosystems of the Middle Taiga of Central Siberia. *Siberian Forest Journal*, (3), pp. 37–53. https://doi.org/10.15372/SJFS20240305 (in Russian).
9. Romanovskaya, A.A., ed., 2023. [*Evaluation of Greenhouse Gases Fluxes in Regional Ecosystems of the Russian Federation*]. Moscow: IGKE, OOO Print, 346 p. (in Russian).
10. Kuklev, S.B., Kremenetskiy, V.V., Krylenko, V.V. and Rudnev, V.I., 2022. Digital Model of the "Carbon Test Site in Krasnodar Region" on the Base of SBIO RAS (Gelendzhik). *Hydrosphere Ecology*, (1), pp. 18–28. https://doi.org/10.33624/2587-9367-2022-1(7)-18-28 (in Russian).
11. Varvarova, A.O., Polukhin, A.A., Berdnikova, E.K., Mukhametov, S.S., Borisenko, G.V. and Pronina, Yu.O., 2023. Spatial and Temporal Variability of Carbonate System Parameters at the Gelendzhik Carbon Test Area During the Summer Period. In: MSU,

2024. *Conference Proceedings of the XII International conference "Marine Research and Education" MARESEDU-2023. Moscow, 23–27 October 2023*. Tver: PoliPRESS. Vol. II(IV), pp. 503–507 (in Russian).

12. Rudnev, V.I., Pushkin, V.V. and Kuklev, S.B., 2024. Methodology for Measuring Greenhouse Gas Concentrations at a Test Site near the Blue Bay (Northeast of the Black Sea). *Hydrosphere Ecology*, (2), pp. 91–100. https://doi.org/10.33624/2587-9367-2024-2(12)-91-100 (in Russian).
13. Wutzler, T., Lucas-Moffat, A., Migliavacca, M., Knauer, J., Sickel, K., Sigut, L., Menzer, O. and Reichstein, M., 2018. Basic and Extensible Post-Processing of Eddy Covariance Flux Data with REddyProc. *Biogeosciences*, 15(16), pp. 5015–5030. https://doi.org/10.5194/bg-15-5015-2018
14. Reichstein, M., Falge, E., Baldocchi, D., Papale, D., Aubinet, M., Berbigier, P., Bernhofer, C., Buchmann, N., Gilmanov, T. et al., 2005. On the Separation of Net Ecosystem Exchange into Assimilation and Ecosystem Respiration: Review and Improved Algorithm. *Global Change Biology*, 11(9), pp. 1424–1439. https://doi.org/10.1111/j.1365-2486.2005.001002.x
15. Lasslop, G., Reichstein, M., Papale, D., Richardson, A.D., Arneth, A., Barr, A., Stoy, P. and Wohlfahrt, G., 2010. Separation of Net Ecosystem Exchange into Assimilation and Respiration Using a Light Response Curve Approach: Critical Issues and Global Evaluation. *Global Change Biology*, 16(1), pp. 187–208. https://doi.org/10.1111/j.1365-2486.2009.02041.x
16. Foken, T. and Wichura, B., 1996. Tools for Quality Assessment of Surface-Based Flux Measurements. *Agricultural and Forest Meteorology*, 78(1-2), pp. 83–105. https://doi.org/10.1016/0168-1923(95)02248-1
17. Timokhina, A.V., Prokushkin, A.S. and Panov, A.V., 2014. Daily and Seasonal Dynamics of CO_2 and CH_4 Concentration in the Atmosphere over the Western Siberia (Pri-Yeniseysk Part) Ecosystems. *Bulletin of KSAU*, (12), pp. 83–88 (in Russian).
18. Rastogi, B., Berkelhammer, M., Wharton, S., Whelan, M.E., Meinzer, F.C., Noone, D. and Still, C.J., 2018. Ecosystem Fluxes of Carbonyl Sulfide in an Old-Growth Forest: Temporal Dynamics and Responses to Diffuse Radiation and Heat Waves. *Biogeosciences*, 15(23), pp. 7127–7139. https://doi.org/10.5194/bg-15-7127-2018
19. Gulev, S.K. and Olchev, A.V., eds., 2025. [*Carbon Polygons: Monitoring, Geoinformation Systems, Sequestering Methods*]. Moscow: Nauchny Mir, 419 p. (in Russian).
20. Stagakis, S., Feigenwinter, C., Vogt, R., Brunner, D. and Kalberer, M., 2023. A High-Resolution Monitoring Approach of Urban CO_2 Fluxes. Part 2 – Surface Flux Optimisation Using Eddy Covariance Observations. *Science of the Total Environment*, 903, 166035. https://doi.org/10.1016/j.scitotenv.2023.166035

Submitted 16.09.2025; accepted after review 11.11.2025;
revised 18.12.2025; published 31.03.2026

About the authors:

Boris V. Divinsky, Leading Researcher, Laboratory of Geology and Lithodynamics, Shirshov Institute of Oceanology, Russian Academy of Sciences (36, Nakhimov Ave., Moscow, 117997, Russia), PhD (Geogr.), **ORCID: 0000-0002-2452-1922, ResearcherID: C-7262-2014**, *divin@ocean.ru*

Sergey B. Kuklev, Head of the Laboratory of Hydrophysics and Modeling, Shirshov Institute of Oceanology, Russian Academy of Sciences (36, Nakhimov Ave., Moscow, 117997, Russia), PhD (Geogr.), **ORCID: 0000-0003-4494-9878, ResearcherID: G-5656-2017**, *kuklev@ocean.ru*

Vyacheslav V. Kremenetsky, Deputy Director for Physical Direction, Shirshov Institute of Oceanology, Russian Academy of Sciences (36 Nakhimov Ave., Moscow, 117997, Russia), PhD (Geogr.), *sk@ocean.ru*

Andrey A. Nedospasov, Junior Researcher, Laboratory of Experimental Ocean Physics, Shirshov Institute of Oceanology, Russian Academy of Sciences (36, Nakhimov Ave., Moscow, 117997, Russia), *nedospasov.aa@ocean.ru*

Vladimir V. Ocherednik, Researcher, Laboratory of Hydrophysics and Modeling, Shirshov Institute of Oceanology, Russian Academy of Sciences (36 Nakhimov Ave., Moscow, 117997, Russia), **ORCID: 0000-0002-3593-7114, ResearcherID: G-2850-2017,** *poekperementarium@gmail.com*

Olga N. Kukleva, Researcher, Laboratory of Hydrophysics and Modeling, Shirshov Institute of Oceanology, Russian Academy of Sciences (36, Nakhimov Ave., Moscow, 117997, Russia), **ResearcherID: J-7126-2018,** *kukleva-ola@mail.ru*

Contribution of the authors:

Boris V. Divinsky – problem statement, analysis of the results, article preparation

Sergey B. Kuklev – problem statement, analysis of the literature sources

Vyacheslav V. Kremenetsky – experiment support

Andrey A. Nedospasov – experiment support

Vladimir V. Ocherednik – experiment support

Olga N. Kukleva – preparation of source data, article preparation

All the authors have read and approved the final manuscript.